

Figure 3 Measured axial ratios of the fabricated antenna proposed in Figure 1 at the boresight angle compared with the numerical results with different air-gap sizes. [Color figure can be viewed in the online issue, which is available at wileyonlinelibrary.com]

etched on a grounded dielectric slab with no vertical vias. The unit cell specification of the AMC ground plane is $w = 12.8$ mm, $g = 0.5$ mm, $h_1 = h_2 = 1.57$ mm, and $\epsilon_r = 2.5$. The reflection phase of the unit cell is zero at the frequency of 4.5 GHz. Because of the removal of the straight part, the probe feed is located at the starting point of the spiral part at $r_0 = 6.36$ mm, where the spiral parameter is $a = 0.3375$ mm/rad. The angle α , defined above, changes from 5π to 6.42π .

The air gap is the result of the sandwiching process of the two layers of dielectric slabs, as shown in Figure 1. The effect of this air gap on the axial ratios of the proposed antenna will be studied in next section.

3. RESULTS

The proposed antenna shown in Figure 1 was simulated using Ansoft High Frequency Simulation Structure (HFSS). The resulting axial ratios are shown in Figure 2 when there is no air gap between the layers. The operating frequency is 4.5 GHz. As can be seen, the antenna exhibits nearly perfect CP performance at the boresight angle, i.e., $\theta = 0^\circ$. The 3-dB axial ratio beamwidth is close to $\pm 30^\circ$. The frequency behavior of the antenna is also studied. The boresight axial ratios versus frequency are plotted in Figure 3 for different air-gap sizes. The center operating frequency of the antenna will increase as the air gap size varies from 0 to 0.3 mm. However, the larger the air-gap size, the narrower the 3-dB frequency bandwidth. To verify numerical results, one prototype antenna with the air-gap size of 0.3 mm was fabricated and tested. The measurement result is also shown in Figure 3. A good agreement is observed between the measurement and numerical results with the same air-gap size of 0.3 mm. The impact of the air-gap

TABLE 1 Minimum Axial Ratios of the Proposed Antenna Shown in Figure 1 at the Boresight Angle for Different Air Gap Sizes

Air Gap (mm)	Axial Ratio (dB) at $\theta = 0^\circ$	Frequency (GHz)
0.000	0.20	4.50
0.100	1.37	4.75
0.200	1.67	4.80
0.300	2.15	4.80
0.400	1.34	5.10

size on the center operating frequency of the proposed antenna is also studied. The results are summarized in Table 1. As can be seen, the air-gap sizes of 0.2 and 0.4 mm will change the center operating frequency to 4.8 and 5.1 GHz, respectively, when compared with the original 4.5 GHz for the 0 air gap. As a result, the center operating frequency of such a low-profile antenna can be tuned by changing the air-gap size between the layers.

4. CONCLUSIONS

The impact of air gap on axial ratios of the low-profile spiral antenna over an AMC ground plane was presented. It was shown that the center operating frequency of the antenna can be controlled by small change in the air-gap size. Numerical and measured results agreed quite well.

REFERENCES

1. L. Shafai, Some array applications of the curl antenna, *Electromagnetics* 20 (2000), 271–293.
2. F. Yang and Y. Rahmat-Samii, Curl antennas over electromagnetic band-gap surface: A low profiled design for CP applications, *IEEE Antennas and Propagation Society International Symposium*, Boston, MA, July 2001, Vol. 3, pp. 372–375.
3. H. Nakano, M. Ikeda, K. Hitosugi, J. Yamauchi, and K. Hirose, A spiral antenna backed by an electromagnetic band-gap material, *IEEE Antennas and Propagation Society International Symposium*, June 2003, Vol. 4, pp. 482–485.
4. A.M. Mehrbani, Low profile spiral antennas over AMC ground planes, M.Sc. Thesis, University of Manitoba, Winnipeg, Manitoba, Canada, 2008.

© 2011 Wiley Periodicals, Inc.

A SMALL CIRCULARLY POLARIZED TAG ANTENNA ON A HIGH-DIELECTRIC SUBSTRATE

Chihyun Cho,¹ Seungbeom Ahn,² Ikmo Park,³ and Hosung Choo²

¹Satellite Comm. Group, Samsung Thales, 188 Gumi-dong, Bundang-gu, Seongnam, 463-870, Korea

²School of Electronic and Electrical Engineering, Hongik University, 72-1 Sangsu-dong, Mapo-gu, Seoul, 121-791, Korea

³School of Electrical and Computer Engineering, Ajou University, 5 Woncheon-dong, Youngtong-gu, Suwon, 443-749, Korea; Corresponding author: hschoo@hongik.ac.kr

Received 23 December 2011

ABSTRACT: The reading range of a tag antenna usually decreases markedly as the antenna size decreases, because of the antenna's reduced gain. This letter describes the use of circular polarization to reduce the size of a tag antenna without decreasing its reading range. This approach resulted in a 33×33 -mm antenna with a substrate thickness of 4 mm that maintained reading ranges of about 3 m for the antenna in free space and 7 m for the antenna on a metallic surface. © 2011 Wiley Periodicals, Inc. *Microwave Opt Technol Lett* 53:2423–2425, 2011; View this article online at wileyonlinelibrary.com. DOI 10.1002/mop.26270

Key words: ceramic substrate; circular polarization; metallic surface

1. INTRODUCTION

Radio-frequency identification (RFID) systems are widely used in an increasing number of applications, such as supply chains, logistics functions, and retail item management. Small RFID tag antennas that operate efficiently on metallic surfaces are useful

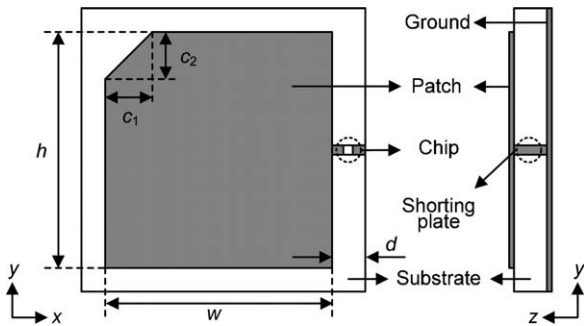


Figure 1 Structure of the proposed CP tag antenna for mounting on metallic objects

in some of these applications. Several designs have been proposed for small tags that can be mounted on metal objects [1, 2]. However, such antennas have a short reading range because their gain is reduced by the reduction in size.

To solve this problem, we applied the concept of circular polarization (CP) to the tag antenna to maintain the reading range even when its size is reduced. The reader antenna radiates CP waves to be able to detect the tag consistently, independent of the tag's position. If a CP tag is used in a RFID system, the reading range can be increased by boosting the polarization efficiency between the reader and the tag antennas. When we used a 33×33 -mm microstrip patch with CP radiation, the resulting tag antenna had a reading range of 7.24 m with a commercial tag chip when it was attached to a 12×12 -cm metallic surface, and a reading range of 2.99 m in free space.

2. ANTENNA STRUCTURE AND CHARACTERISTICS

Figure 1 shows the proposed small CP tag antenna. The radiation patch was printed on a high-dielectric ceramic substrate ($\epsilon_r = 28$, $\tan \delta = 0.001$) and the upper-left corner was truncated by $c_1 \times c_2$ to produce right-hand circular polarization (RHCP). The impedance of a tag chip is generally capacitive and the tag antenna should thus have inductive input impedance for conjugate matching with the chip. In the proposed structure, the radiating patch and the ground were connected by a thin line to produce suitable self-inductance. The tag chip was placed in the middle of the thin line for easy installation. We optimized the detailed design parameters using the Pareto genetic algorithm with the FEKO EM simulator. In the optimization process, the tag antenna was optimized as a conjugate match with the tag chip as well as having RHCP radiation characteristics. The opti-

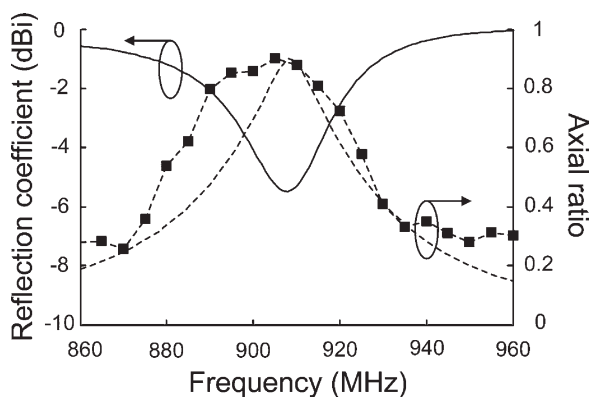


Figure 2 Reflection coefficient and AR of the proposed CP tag antenna —: S_{11} : simulated AR ---■---: measured AR

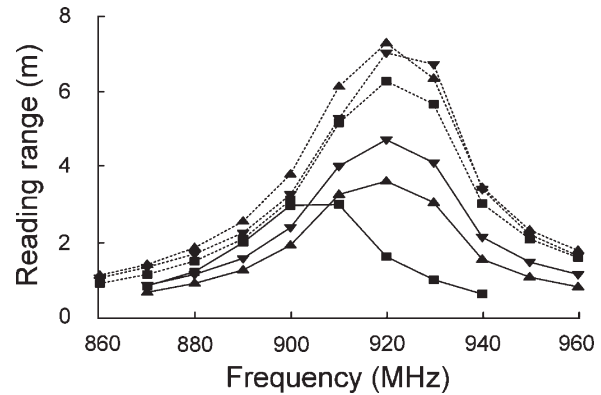


Figure 3 Reading range —■—: free space —▲—: 6-cm ground —▼—: 8-cm ground■.....: 10-cm ground▲.....: 12-cm ground▼.....: 20-cm ground

mized parameters were $w = 29.02$ mm, $h = 30.28$ mm, $c_1 = 5.73$ mm, $c_2 = 0.78$ mm, and $d = 3.46$ mm.

Figure 2 shows the reflection coefficient and axial ratio (AR) of the proposed antenna, measured using a network analyzer (Agilent E5071A), which supports the measurement of balanced-feed systems. The impedance of the tag chip was about $(20 - j150) \Omega$ at the operating frequency. The measured reflection coefficient indicated a half-power bandwidth of 896–918 MHz. Figure 2 shows the AR using a dashed line, where +1, 0, and -1 signify RHCP, linear polarization (LP) and left-hand circular polarization (LHCP), respectively. The proposed CP tag antenna exhibited an AR greater than 0.7 (~ 3 dB) from 890 to 920 MHz.

Next, we measured the reading range of the proposed tag antenna using a commercial RFID system with a RFID tag chip (Higgs-2, Alien). The reader system transmitted a power of 1 W using a RHCP reader antenna. Figure 3 shows the reading range where the tag was attached to various ground plates. As expected, the maximum reading range in free-space (■) occurred at 910 MHz, coincident with the high value of AR shown in Figure 2. The reading range decreased as the frequency deviated from 910 MHz, due to impedance and polarization mismatches.

We attached the tag to metallic surfaces (6×6 , 8×8 , 10×10 , 12×12 , and $20 \text{ cm} \times 20 \text{ cm}$) using double-sided adhesive tape and then measured the reading ranges. The maximum reading range increased as the size of the metallic surface increased. Interestingly, the reading range did not change significantly as the size of the metallic surface increased beyond 12 cm. This result indicates that even when the ground plate is larger than 1λ , the reading range can be maintained at greater than 7 m.

We also measured the reading range of the LP tag to compare it with that of the CP tag. The reading range of the LP tag was reduced by half although other conditions, such as impedance, reader antenna, and ground size were the same as with the CP tag. This result clearly shows that the reading range can be doubled using a CP tag.

3. OPERATING PRINCIPLES

The scattering of an antenna is normally divided into a structural mode and an antenna mode. The antenna mode is produced by the radiating parts with the same polarization as the incident wave, while the structural mode is derived from the remaining parts, such as the ground plate and the substrate with the reversed polarization. Figure 4 shows the AR responses of the structural and antenna modes of the proposed CP tag.

The structural mode was obtained from the backscattered field when the tag antenna was fully matched to the tag chip.

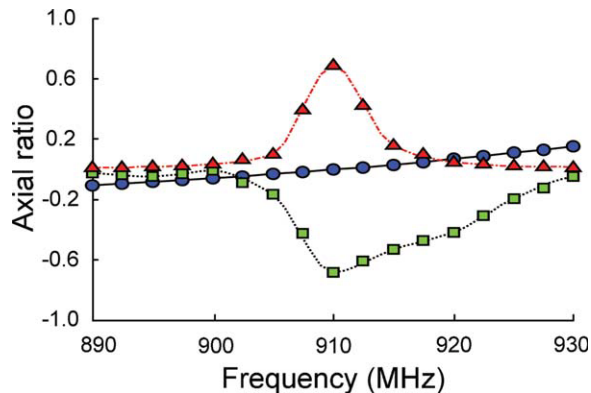


Figure 4 AR of various modes —●—: backscattering of the shorted tag antenna —▲—: antenna mode —■—: structural mode. [Color figure can be viewed in the online issue, which is available at wileyonlinelibrary.com]

The antenna mode was then calculated by subtracting the structural mode from the backscattering of the shorted tag antenna [3]. As expected, the structural mode exhibited reversed polarization (close to $AR = -1$) near 910 MHz, while the antenna mode showed the same polarization (close to $AR = 1$) as the incident field. This result demonstrated that polarization mismatch did not occur between the CP tag and the reader antenna, and that the CP tag produced an increased reading range [4].

4. CONCLUSIONS

We have developed a miniaturised CP tag antenna without compromising its reading range. The antenna had 3-dB bandwidth of 896–918 MHz even though its size was $33 \text{ mm} \times 33 \text{ mm} \times 4 \text{ mm}$. The maximum reading range was 7 m, which was twice that of the same size of LP tag.

REFERENCES

1. J.-Y. Park and J.-M. Woo, Miniaturized dual-band S-shaped RFID tag antenna mountable on metallic surface, *Electron Lett* 44 (2008), 1339–1341.
2. S.-L. Chen, A miniature RFID tag antenna design for metallic objects application, *IEEE Antenn Wireless Propag Lett* 8 (2009), 1043–1045.
3. W.L. Stutzman and G.A. Thiele, *Antenna theory and design*, Wiley, NY, 2002.
4. C. Cho, I.Park, and H.Choo, Design of a circularly polarized tag antenna for increased reading range, *IEEE Trans Antenn Propag Lett* 57 (2009), 3418–3422.

© 2011 Wiley Periodicals, Inc.

A LONG-PERIOD GRATING WRITTEN IN THE CLADDING OF AN OPTICAL FIBER

Tianfu Jiang

School of Computer Science, Civil Aviation Flight University of China, Guanghan, Sichuan 618307, China; Corresponding author: jtffhbj@sina.com

Received 23 December 2010

ABSTRACT: A long-period grating (LPG) written in the cladding of an optical fiber is demonstrated. The optical fiber is specially designed and manufactured, which cladding is photosensitive, and core is not. The cladding LPG is written in by illuminating a cladding photosensitive fiber with an UV lamp through an amplitude grating mask. The cladding

LPG is compared with a core LPG manufactured in the same way, and the property of the cladding LPG is different from that of the core LPG. © 2011 Wiley Periodicals, Inc. *Microwave Opt Technol Lett* 53:2425–2427, 2011; View this article online at wileyonlinelibrary.com. DOI 10.1002/mop.26269

Key words: long-period grating; cladding grating

1. INTRODUCTION

The discovery of photosensitivity in Ge-doped optical fiber has led to an important technique that a fiber grating can be written in the core of the optical fiber. Photosensitivity was firstly observed by Hill et al. [1], and practical fiber gratings were first demonstrated by Meltz et al. [2]. From that time, many kinds of fiber gratings have been written in optical fibers, including Bragg gratings, long-period gratings (LPGs), titled fiber gratings, chirped gratings, etc. On the other hand, many techniques have been developed to write gratings, such as the hydrogen-loading technique [3], the mask-writing technique [4], and the high-doped Ge technique [5], etc. The wavelength of the writing laser can be 248 nm, 244 nm, 266 nm, 193 nm, and 157 nm, etc. However, all fiber gratings were written in the core of the fiber.

After LPGs were proposed [6], some methods were demonstrated to create LPGs, which do not use an ultraviolet (UV) laser as the writing light source. Researchers found that periodic heating or bending can also induce LPGs in fibers. Thus a CO_2 laser operating at the wavelength of $10.7 \mu\text{m}$ was also used to write LPGs using a point-by-point writing technique [7]. These LPGs are believed to be induced by periodic bending when irradiating with the high-power laser. Although the LPG may lie in the core and the cladding at the same time, the periodic bending of the core is the correct explanation for the LPG. Besides, the LPG written by a CO_2 laser has a similar spectrum compared with that written by a UV laser.

In this article, we demonstrate that a LPG can be written in the cladding of a optical fiber. A cladding LPG is compared with a core LPG, showing that they have different spectral property. Because the cladding LPG contact directly with the out environment, the cladding LPG may be used as a chemical, biochemical or biological sensor in future applications, or used to construct new passive components.

2. FABRICATION OF CLADDING LPG

To write a LPG in the cladding of fiber, we must have a specially devised optical fiber, cladding photosensitive fiber (CPF), in which the cladding is photosensitive and the core is not. Thus we need to dope germanium (Ge) in the cladding, and keep the core pure SiO_2 . For a general telecommunication optical fiber, Ge is doped in the core to increase the refractive index of the core, and then total internal reflection ensures that all of the energy is carried in the fiber core. However, if the cladding is doped with Ge and the core is pure SiO_2 , the refractive index in the cladding will be larger than that of the core, and the light cannot be guided down the fiber. To reduce the refractive index of the cladding, boron (B) is co-doped in the cladding, and this reduces the refractive index of the cladding. B co-doped with Ge is also helpful in increasing the photosensitivity [5]. We devised that the doped Ge increases the refractive index difference between the cladding and core by 6%, and the doped B decreases the refractive index difference by 14%. Thus the refractive index of the core is 8% higher than that of the cladding when the cladding is co-doped with Ge and B. The CPF was drawn using the traditional modified chemical vapour deposition technique. The final parameters of the special fiber are: single-